• Clinical Research •

Brain activity in different brain areas of patients with diabetic vitreous hemorrhage according to voxel-based morphometry

Li-Jun Ji[1], Jin-Yu Hu[2,3], Yan-Mei Zeng[2,3], Qian Ling[2,3], Jie Zou[2,3], Cheng Chen[2,3], Liang-Qi He[2,3], Xiao-Yu Wang[2,3], Hong Wei[2,3], Xu Chen[4], Yi-Xin Wang[5], Yi Shao[3,6], Yao Yu[2]

[1]Department of Ophthalmology, Dahua Hospital, Shanghai 200237, China

[2]Department of Endocrine and Metabolic, the First Affiliated Hospital of Nanchang University, Jiangxi Clinical Research Centre for Endocrine and Metabolic Disease, Jiangxi Branch of National Clinical Research Center for metabolic Disease, Nanchang 330006, Jiangxi Province, China

[3]Department of Ophthalmology, the First Affiliated Hospital of Nanchang University, Nanchang 330006, Jiangxi Province, China

[4]Ophthalmology Centre of Maastricht University, Maastricht 6200MS, Limburg Provincie, the Netherlands

[5]School of optometry and vision science, Cardiff University, Cardiff, CF24 4HQ, Wales, UK

[6]Department of Ophthalmology, Shanghai General Hospital, Shanghai Jiao Tong University School of Medicine, National Clinical Research Center for Eye Diseases, Shanghai 200080, China

Co-first authors: Li-Jun Ji and Jin-Yu Hu

Correspondence to: Yao Yu. Department of Endocrinology and Metabolism, Gaoxin Hospital of the First Affiliated Hospital of Nanchang University, Nanchang 330006, Jiangxi Province, China. 375135747@qq.com; Yi Shao. Department of Ophthalmology, Shanghai General Hospital, Shanghai Jiao Tong University School of Medicine, National Clinical Research Center for Eye Diseases, Shanghai 200080, China. freebee99@163.com

Received: 2023-12-30 Accepted: 2024-08-29

Abstract

● **AIM:** To elucidate the neuropathological mechanisms underlying diabetic vitreous hemorrhage (DVH) and its correlation with clinical characteristics.

● **METHODS:** Twenty-one individuals with DVH (male/female 12/9; mean age 52.29±11.66y) were selected, alongside 21 appropriately matched controls with diabetes mellitus (DM). Voxel-based morphometry (VBM) techniques were employed to identify aberrant functional regions in the brain. Receiver operating characteristic (ROC) curves were utilized for classification based on the average VBM values of the two groups, and Pearson correlation analysis was conducted to assess the relationship between average VBM values in distinct brain regions and clinical manifestations.

● **RESULTS:** Relative to the DM controls, DVH patients exhibited reduced VBM values in the right superior temporal pole, the right superior temporal gyrus, the right medial orbital frontal gyrus, and the left superior frontal gyrus. Furthermore, ROC curve analysis of these four brain regions in DVH patients demonstrated a high degree of accuracy, as indicated by the area under the curve. The average VBM value in each of these regions exhibited a negative correlation with both the duration of DVH and the score on the Hospital Anxiety and Depression Scale (HADS).

● **CONCLUSION:** Pathological alterations in four distinct brain regions are observed in patients with DVH, potentially reflecting neuropathological changes associated with this condition.

● **KEYWORDS:** diabetic vitreous hemorrhage; voxel-based morphometry; Hospital Anxiety and Depression Scale; brain areas

DOI:10.18240/ijo.2025.02.09

Citation: Ji LJ, Hu JY, Zeng YM, Ling Q, Zou J, Chen C, He LQ, Wang XY, Wei H, Chen X, Wang YX, Shao Y, Yu Y. Brain activity in different brain areas of patients with diabetic vitreous hemorrhage according to voxel-based morphometry. *Int J Ophthalmol* 2025;18(2):258-267

INTRODUCTION

The vitreous body, an achromatic and lucid ocular tissue, assumes pivotal roles as an integral component of the refractive media and in the stabilization of the retina. Given its absence of intrinsic vasculature, instances of vitreous hemorrhage (VH) commonly emanate from vascular structures or nascent blood vessels situated in adjacent tissues, such as the choroid or retina[1]. Among diabetic patients, the protracted

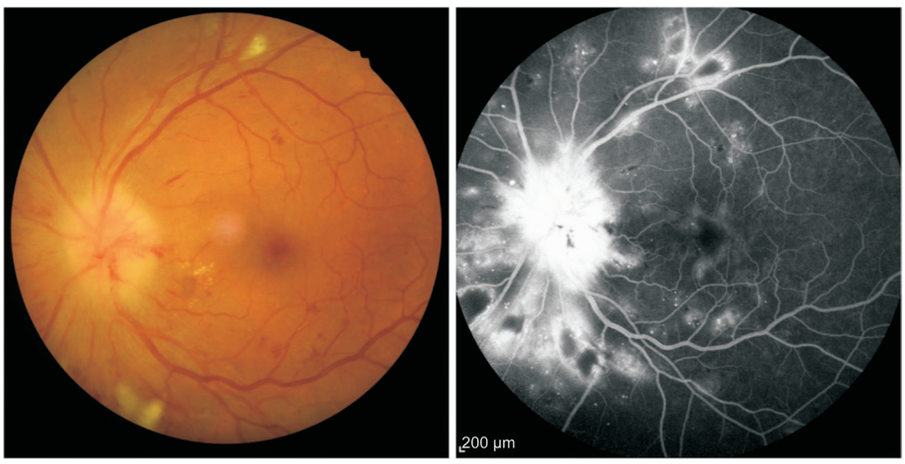

Figure 1 An example of DVH was examined on fundus camera and fluorescence fundus angiography DVH: Diabetic vitreous hemorrhage.

prevalence of hyperglycemia catalyzes polyol metabolism, amplifies oxidative stress levels, inflicts damage upon capillary endothelial cells, incites microthrombus formation with consequential effects on microcirculation, diminishes retinal oxygenation, and prompts the release of retinal cells following stimulation. Diverse growth factors further undermine the blood-retinal barrier, instigating retinal neovascularization[2]. These nascent blood vessels, fragile in nature, are susceptible to rupture, thereby culminating in diabetic vitreous hemorrhage (DVH; Figure 1). While a diminutive VH may gradually undergo absorption, thus restoring vision[3], prolonged retention of accumulated blood poses the risk of intricate complications, including tractional retinal detachment, proliferative retinopathy, cataracts, glaucoma, vitreous atrophy, and other maladies, ultimately leading to irreversible vision impairment. An investigative inquiry revealed that such consequences exert a non-negligible impact on the residents' lives, economy, and education[4], heightening their susceptibility to mortality[5]. Consequently, the early screening and diagnosis of DVH assume a pivotal role in prognosis, facilitating timely intervention, treatment, and subsequent monitoring.

In tandem with fundus photography, ocular ultrasound and fluorescence fundus angiography (FFA) constitute pivotal modalities employed in the clinical identification of VH. Ultrasound detection stands as an indispensable non-invasive adjunctive diagnostic tool for discerning DVH. Employing high-resolution ultrasound facilitates the meticulous examination of the fundus in DVH-afflicted patients, enabling precise localization, assessment of progression, and consideration of various contributory factors. This, in turn, enhances the capacity for nuanced differential diagnosis, prognostication of treatment outcomes, and long-term monitoring. Conversely, FFA, while possessing diagnostic merit in the context of DVH, bears the imprint of invasiveness. Its efficacy is contingent upon the proficiency and dexterity of the operator, as well as the cooperative disposition of the patient. Moreover, these aforementioned methodologies prove notably efficacious in cases of advanced DVH, yet their utility diminishes in the early stages of diagnosis and in unraveling the disease's pathogenesis. Notably, the detection of minute hemorrhages *via* ultrasound may pose challenges, thereby elevating the specter of oversight and jeopardizing the patient's visual acuity.

In recent years, the ubiquity of magnetic resonance imaging technology has burgeoned. As a non-invasive, expedient, high-resolution, and discerning modality, resting-state magnetic resonance imaging (MRI) assumes a distinctive ascendancy in elucidating the anatomical configuration of the targeted tissue. Voxel-based morphometry (VBM), a comprehensively automated whole-brain analytical technique, quantifies alterations in tissue density at the voxel level within individual MRI images[6]. This methodology furnishes a precise and impartial quantitative assessment of variations in the density and volume of cerebral white and gray matter, establishing itself as a dependable cornerstone for intergroup comparisons of anatomical brain structures in the realm of research. Numerous antecedent investigations have availed themselves of VBM technology in the exploration of neurological afflictions, such as depression[7], idiopathic generalized epilepsy[8], Alzheimer's disease[9], schizophrenia[10], and Parkinson's disease. Within the domain of pathology-related research, this modality has catalyzed noteworthy breakthroughs in the study of diverse ophthalmic maladies[11], including but not limited to glaucoma[12], optic neuritis[13], amblyopia[14], strabismus[15], and non-specific blindness[16]. These inquiries have underscored alterations in both the anatomy and functionality of the brain across various pathologies, elucidating the inseparable nexus between visual and cortical function.

Henceforth, the prevailing inquiry availed MRI conjoined with VBM technology for the dissection of cerebral tissue anatomy in patients afflicted with DVH. This endeavor sought to scrutinize alterations within said tissue and apprehend

Table 1 Baseline demographic and clinical data of the study participants

Condition	DVH	DM	*t*	*P*[a]
Male/female	12/9	12/9	N/A	-
Age (y)	52.29±11.66	51.54±10.73	0.276	0.815
Weight (kg)	69.38±10.16	69.82±10.78	0.153	0.911
Handedness	21R	21R	N/A	-
Duration of DVH (d)	23.71±13.76	N/A	N/A	N/A
Best-corrected VA-left eye	0.45±0.20	1.05±0.20	-3.723	0.006
Best-corrected VA-right eye	0.40±0.15	1.00±0.15	-3.764	0.009
Duration of DM (y)	25.53±15.98	24.94±14.63	0.083	0.903
HbA1c (%)	6.12±0.52	4.71±0.65	0.162	0.826

[a]*P*<0.05 independent *t*-tests comparing two groups. Chi-square test for gender and handedness. DVH: Diabetic vitreous hemorrhage; N/A: Not applicable; VA: Visual acuity; DM: Diabetes mellitus.

the correlation existing between these changes and clinical manifestations. Although individuals grappling with diabetic VH do not manifest overt or severe ocular discomfort, modifications in visual acuity facilely instigate perturbations in the patient's affective state. Myriad investigations have transcended the confines of simplistic exploration into the etiology of ocular maladies, instead directing attention towards their impact on life quality and psychological well-being. We postulate a discernible nexus between emotional vicissitudes in patients and the malady. To delve deeper into this conjecture, the Hospital Anxiety and Depression Scale (HADS) was employed. In summation, the ultimate purview of this research resides in furnishing insights for the premature identification and diagnosis of DVH, thereby forestalling its progression towards irreversible visual debilitation.

PARTICIPANTS AND METHODS

Ethical Approval This investigation adhered rigorously to the tenets of medical ethics, aligning itself with the precepts articulated in the Declaration of Helsinki, and received the imprimatur of the Medical Ethics Committee at the First Affiliated Hospital of Nanchang University (ethics approval number: 2021039). All conscientious participants, acting as volunteers, were apprised of the study's objectives, methodologies, and conceivable outcomes, duly manifesting their understanding and consent through signed confirmation.

Participants A total of 21 type-2 diabetic patients with VH were recruited at the First Affiliated Hospital of Nanchang University from October 2021 to September 2023 in the present study, where the doctors identified the disease during treatment and recommended the project researchers to discuss informed consent. Among these patients, comprise 12 males and 9 females, and the age was expressed as mean±standard deviation (SD). They were enlisted in the experimental group based on the subsequent criteria: 1) dextral inclination; 2) adjudicated with type 2 diabetes mellitus (DM); 3) unblemished ocular antecedence antecedent to DVH manifestation; 4) VH not ascribed to alternate factors such as ocular trauma; 5) VH diagnosis substantiated through employment of a fundus camera concomitant with FFA; 6) Absence of any other ocular maladies (*e.g.*, glaucoma or amblyopia) in either ocular organ; 7) absence of cerebral parenchymal irregularities.

The eligibility criteria for enlisting subjects with DM were as follows: 1) exclusive right-handedness; 2) adjudicated with type 2 DM; 3) equitable distribution of gender, age, weight, and duration of diabetes comparable to the DVH group (Table 1); 4) optimal best-corrected visual acuity (BCVA) exceeding 1.0 (decimal) in both ocular entities.

Within the two groups, individuals presenting with the subsequent conditions were systematically omitted: 1) any antecedent of ocular surgical interventions; 2) a history of traumatic ocular incidents; 3) miscellaneous physical aberrations encompassing cardiovascular maladies and hypertensive states; 4) protracted exposure to substances, namely drugs, tobacco, or alcoholic beverages; 5) discernible aberrations upon cerebral imaging; 6) instances of untimely parturition; 7) any elements exerting influence on VBM measurements, inclusive of suboptimal collaboration or the presence of metallic implants within the corporeal framework.

Magnetic Resonance Imaging Parameters The three-Tesla MR scanner (Trio; Siemens, Munich, Germany) was employed for MRI scanning. Functional images were acquired using a spoiled gradient-recalled echo sequence. The parameters were as follows: repetition time=1900ms, echo time=2.26ms, flip angle=9°, thickness=1.0 mm, field of view=250×250 mm, gap=0 mm, and in-plane resolution=256×256. In the culmination of the procedure, a total of 176 images and 240 functional volumes were meticulously obtained, with a repetition time of 2000ms, echo time of 30ms, flip angle of 90°, slice thickness of 4.0 mm, field of view=220×220 mm, gap=1.2 mm, in-plane resolution=64×64, and 29 axial slices.

Voxel-Based Morphometry Analysis Initially, we employed the MRIcro software to eliminate incomplete data. Subsequently, the Voxel-Based Morphometry toolbox (VBM8) (http:// dbm.neuro.uni-jena.de/vbm8/), Statistical Parametric Mapping (SPM8; http://www.fil.ion.ucl.ac.uk), and MATLAB 7.9.0 software (R2009b; The Mathworks, Inc., Natick, MA, USA) were employed for the processing of all structural images. The cerebral structures underwent segmentation into white matter, gray matter, and cerebrospinal fluid, utilizing the default estimation options (with a 60-mm cut-off for estimating the Gaussian smoothness of bias in image intensity) and the International Consortium for Brain Mapping (ICBM) European template for initial affine transformation within VBM8.

Employing the exponential lie algebra (DARTEL) method embedded in diffeomorphic anatomical registration in VBM8, we standardized the white and gray matter components of the cerebral structures to align with the Montreal neurological institute (MNI) standard space. Ultimately, we applied a 6-mm full-width-at-half-maximum (FWHM) gaussian kernel to smooth the modulated volumes and presented the modulated, normalized, and smoothed images for group-level analyses.

Statistical Analysis A comprehensive examination of the General Linear Model (GLM) was undertaken utilizing the SPM8 toolkit (http://www.fil.ion.ucl.ac.uk/spm). To discern differentials in Gray Matter Volume (GMV) and White Matter Volume (WMV) between the two cohorts, a two-sample *t*-test was executed employing the Resting-State fMRI Data Analysis Toolkit (REST; http://www.restfmri.net). Gaussian Random Field (GRF) theory, specifically chosen for its efficacy in multiple comparison correction, governed the statistical analysis (GRF corrected, minimum z>2.3, voxel level $P<0.001$, cluster level $P<0.05$). The amalgamation of total intracranial volumes from all volunteers into the design matrix facilitated global calculations, thus mitigating global nuisance effects. For the generation of authentic data maps, the voxel threshold was expansively set to encompass 20 contiguous voxels, and a chromatic representation ensued through the overlay of statistically significant voxels onto the 3DT1 weighted normalized images[17-18]. All subjects within the experimental cohort satisfactorily completed the HADS, and subsequent correlation analyses were executed as delineated below.

Brain Behavior Utilizing the REST software, we delineated cerebral regions exhibiting distinct VBM values, designating them as Regions of Interest (ROI) within the dichotomous groups. Subsequently, we regarded the ascertained average GMV value across all voxels as the representative VBM value for each distinct ROI. Moreover, we conducted correlation analyses to elucidate the associations between the mean VBM values of diverse cerebral regions within the DVH cohort and pertinent metrics, including HADS scores, the temporal extent of DVH manifestation, and the mean VBM value itself. A significance threshold of $P<0.05$ was applied to discern statistically meaningful relationships.

Clinical Data Analysis All the clinical data from the volunteers were systematically amassed, encompassing the temporal extent of DVH affliction, the acuity of BCVA, and the demographic variables. The comparative analysis between the two cohorts was executed employing SPSS 26.0 software (SPSS, Chicago, IL, USA), employing the independent sample *t*-test. A significance threshold of $P<0.05$ was established to demarcate a statistically noteworthy distinction.

Receiver Operating Characteristic Analysis A receiver operating characteristic (ROC) curve was delineated for the juxtaposition of data emanating from distinct cerebral regions, thereby facilitating a statistical evaluation of the mean redistribution quotient of VBM across four interconnected cerebral loci.

Correlation Analysis In the analysis of each patient afflicted with DVH, correlation examinations were employed to ascertain the association between the mean VBM values within four distinct cerebral regions among the DVH cohort and two clinical parameters: the temporal span since the diagnosis of DVH, and the HADS score. $P<0.05$ was deemed indicative of statistical significance.

RESULTS

Demographic Information No statistically significant distinctions manifested between the two cohorts concerning age, weight, duration of malaise, or glycosylated hemoglobin levels ($P<0.05$). The examination of gender and handedness through the Chi-square test is delineated in Table 1.

Voxel-Based Morphometry Values In contrast to the dorsomedial regions, the VBM measurements within the right superior temporal pole, right superior temporal gyrus, right medial orbital frontal gyrus, as well as the left superior frontal gyrus (SFG) exhibited a noteworthy and statistically significant reduction in individuals diagnosed with DVH ($P<0.001$, adjusted for multiple comparisons; Figures 2 and 3, Table 2).

Correlation Analysis In individuals afflicted with DVH, VBM values within the quadrilateral cerebral domains (namely, the right superior temporal pole, right superior temporal gyrus, right medial orbital frontal gyrus, and left SFG) exhibited an inverse correlation with the temporal progression of the ailment ($r=-0.4634$, $P=0.0007$; $r=-0.6212$, $P<0.0001$; $r=-0.3508$, $P=0.0047$; $r=-0.4695$, $P=0.0006$, respectively; Figure 4). The VBM metrics pertaining to the aforementioned cerebral locales further demonstrated a negative correlation with HADS scores ($r=-0.6768$, $P<0.0001$; $r=-0.8631$, $P<0.0001$; $r=-0.4157$, $P=0.0016$; $r=-0.6575$, $P<0.0001$; Figure 5).

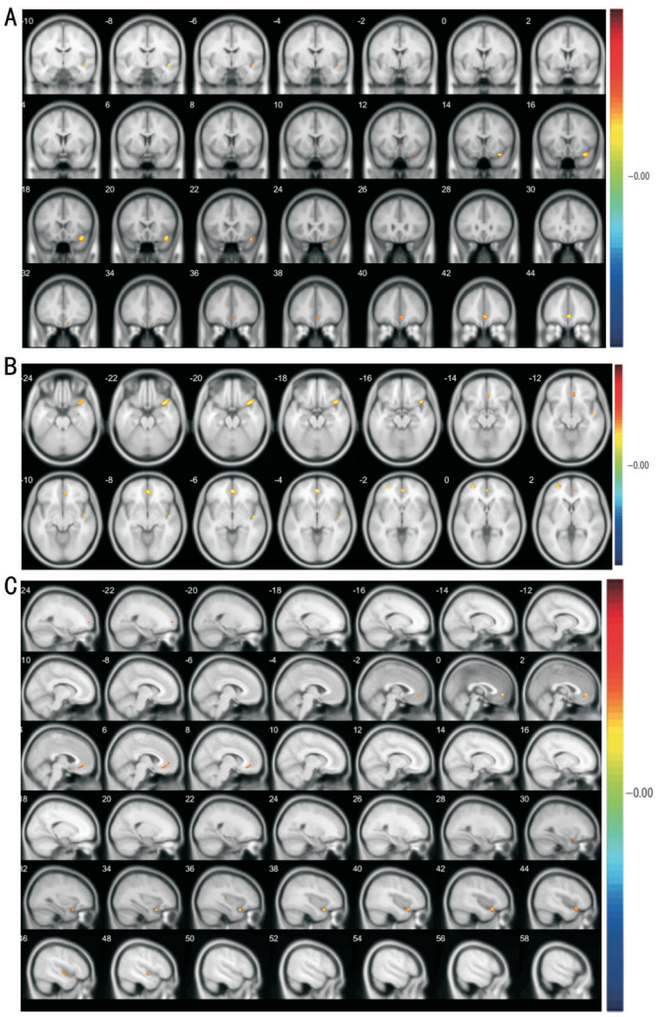

Figures 2 Spontaneous brain activity in DVH and DM Significant differences in VBM values between DVH patients and DM. The brain regions with different VBM values were the right superior temporal pole, right superior temporal gyrus, right medial orbital frontal gyrus as well as left superior frontal gyrus. VBM: Voxel-based morphometry; DVH: Diabetic vitreous hemorrhage; DM: Diabetes mellitus controls.

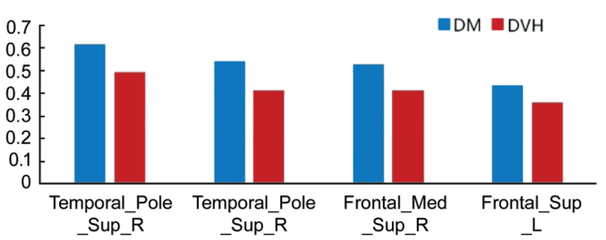

Figure 3 The average VBM values of DVH patients and DM Compared with the DMs, the voxel-based morphometry values in the Temporal_ Pole_Sup _R, Temporal_Sup_R, Frontal_Med_Orb_R, Frontal_Sup_L of DVH patients were all significantly decreased. Temporal_Pole_Sup_R: Right superior temporal pole; Temporal_Sup_R: Right superior temporal gyrus; Frontal_Med_Orb_R: Right medial orbital frontal gyrus; Frontal_ Sup_L: Left superior frontal gyrus; VBM: Voxel-based morphometry; DVH: Diabetic vitreous hemorrhage; DM: Diabetes mellitus controls.

Receiver Operating Characteristic Curves ROC curves were employed to scrutinize the mean values derived from

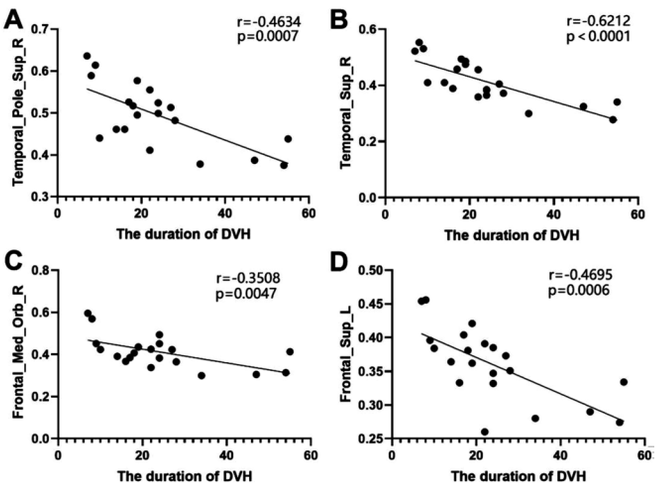

Figure 4 Correlation analysis between the disease of DVH patients duration and the VBM values of the Temporal_Pole_Sup_R, Temporal_ Sup_R, Frontal_Med_Orb_R, Frontal_Sup_L Voxel-based morphometry values in all four brain regions (right superior temporal pole, right superior temporal gyrus, right medial orbital frontal gyrus, and left superior frontal gyrus) were negatively correlated with disease duration (*r*=-0.4634, *P*=0.0007; *r*=-0.6212, *P*<0.0001; *r*=-0.3508, *P*=0.0047; *r*=-0.4695, *P*=0.0006, respectively). VBM: Voxel-based morphometry; DVH: Diabetic vitreous hemorrhage; DM: Diabetes mellitus controls.

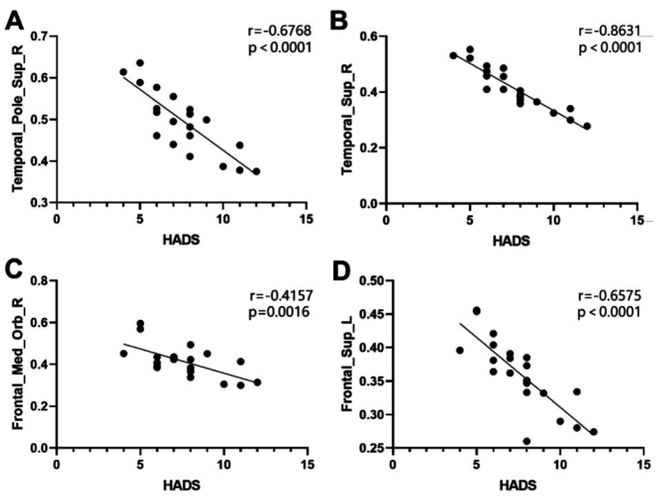

Figure 5 Correlation analysis between HADS scores and the VBM values of the Temporal_Pole_Sup_R, Temporal_Sup_R, Frontal_ Med_Orb_R, Frontal_Sup_L VBM values of the above four brain regions were also negatively correlated with HADS scores (*r*=-0.6768, *P*<0.0001; *r*=-0.8631, *P*<0.0001; *r*=-0.4157, *P*=0.0016; *r*=-0.6575, *P*<0.0001). VBM: Voxel-based morphometry; DVH: Diabetic vitreous hemorrhage; DM: Diabetes mellitus controls.

VBM across the four cerebral regions. The computed areas beneath the curves manifested as follows: 0.905 (*P*<0.0001; 95%CI: 0.807-1.000) for the right superior temporal pole, 0.892 (*P*<0.0001; 95%CI: 0.795-0.988) for the right superior temporal, 0.884 (*P*<0.0001; 95%CI: 0.768-0.999) for the right medial orbital frontal, and 0.899 (*P*<0.0001; 95%CI: 0.797-1.000) for the left SFG (Figure 6).

Table 2 Brain areas with significantly different voxel-based morphometry values between two groups

Brain areas	BA	MNI coordinates			Number of voxels	*T* value	ROI order
		X	Y	Z			
DVH<DM	-						
Temporal_Pole_Sup_R	38	34.5	15	-21	303	6.2692	1
Temporal_Sup_R	-	46.5	-9	-7.5	70	6.0291	2
Frontal_Med_Orb_R	10	1.5	46.5	-3	243	6.4316	3
Frontal_Sup_L	8	-30	54	0	83	5.9227	4

The statistical threshold was set at the voxel level with $P<0.001$ for multiple comparisons using Gaussian random field (GRF) theory (GRF corrected, minimum $Z>2.3$, voxel level $P<0.001$, cluster level $P<0.05$). MNI: Montreal Neurological Institute; BA: Brodmann area; DVH: Diabetic vitreous hemorrhage; DM: Diabetes mellitus controls; Temporal-Pole-Sup-R: Right superior temporal pole; Temporal-Sup-R: Right superior temporal gyrus; Frontal-Med-Orb-R: Right medial orbital frontal gyrus; Frontal-Sup-L: Left superior frontal gyrus; ROI: Regions of interest.

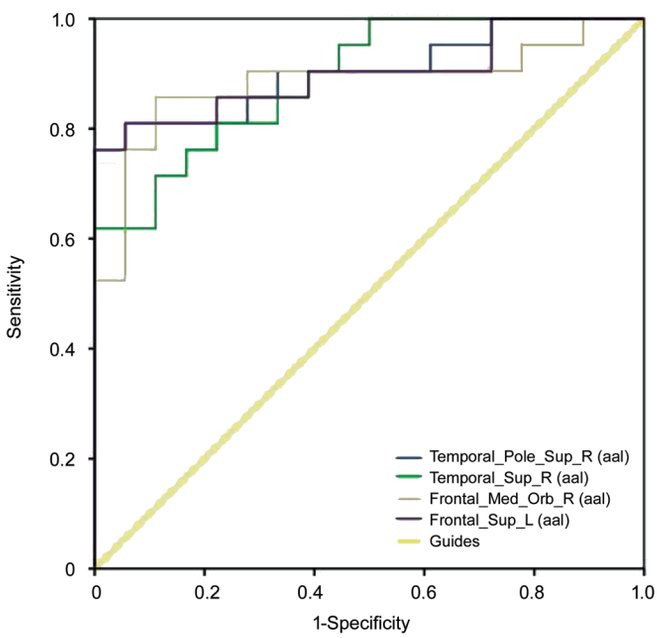

Figure 6 ROC curve of the VBM values in altered brain areas The areas under the curves were 0.905 ($P<0.0001$; 95%CI: 0.807-1.000) for right superior temporal pole, 0.892 ($P<0.0001$; 95%CI: 0.795-0.988) for right superior temporal, 0.884 ($P<0.0001$; 95%CI: 0.768-0.999) for right medial orbital frontal; and 0.899 ($P<0.0001$; 95%CI: 0.797-1.000) for left superior frontal gyrus. VBM: Voxel-based morphometry; DVH: Diabetic vitreous hemorrhage; DM: Diabetes mellitus controls.

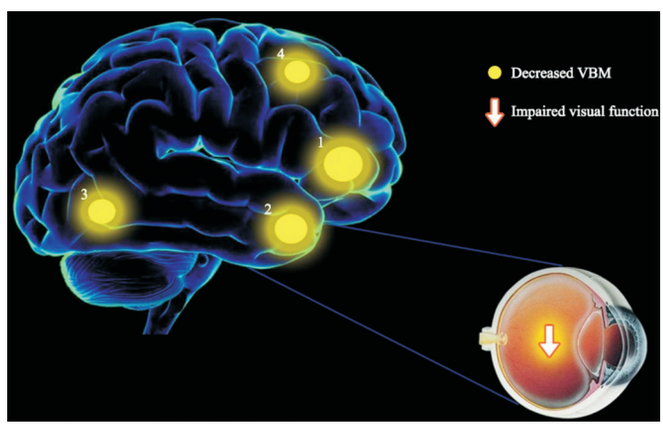

Figure 7 VBM value in each region of DVH patients Compared with the DM, the voxel-based morphometry values in the in the following regions were decreased to various extents: 2-Temporal_Pole_Sup_R, 3-Temporal_Sup_R, 1-Frontal_Med_Orb_R, 4-Frontal_Sup_L of DVH patients were all significantly decreased. VBM: Voxel-based morphometry; DVH: Diabetic vitreous hemorrhage; DM: Diabetes mellitus controls.

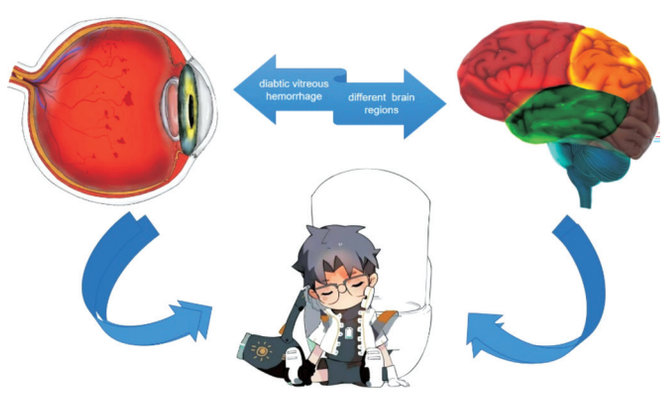

Figure 8 Relationship between VBM values and emotional state The VBM values were decreased in many specific regions in DVH patients compared with the DM, and DVH patients seem more likely to produce anxiety and depression. VBM: Voxel-based morphometry; DVH: Diabetic vitreous hemorrhage; DM: Diabetes mellitus controls.

DISCUSSION

This pioneering investigation employs the VBM methodology to scrutinize aberrations within cerebral regions among individuals afflicted with DVH. Our discernment reveals diminished VBM metrics in the right superior temporal pole, right superior temporal gyrus, right medial orbital frontal gyrus, and left SFG in DVH subjects in comparison to their counterparts. Remarkably, guided by the discerning ROC curve-derived evidence, the precision of the identified cerebral regions stands notably robust, with particular emphasis on the right superior temporal pole. Furthermore, a discernible negative correlation is discerned between the average VBM value within each specified region and both the temporal extent of the ailment and the HADS score. Specifically, heightened disease duration or elevated HADS scores indicative of increased anxiety and depression precipitate a concomitant reduction in VBM, as visually depicted in Figures 7 and 8.

The temporal pole (TP), identified also as the quasi-limbic area[19], resides anatomically adjacent to the amygdala within the limbic system and the orbitofrontal cortex (OFC). It serves as a pivotal conduit of information linking these two domains, exhibiting functional and characteristic parallels with the limbic system. Notably, the TP encompasses elements such as the amygdala and orbital frontal cortex absent in the auditory, visual, and olfactory channels, thereby segregating them from the sensory periphery[20]. In contradistinction to the superior temporal sulcus, renowned for its responsiveness to biological movement and gaze direction, the TP exhibits heightened sensitivity when paired with intricate social stimuli presented in the form of narrative or text[21].

In their scrutiny of macaques, Martin *et al*[22] discerned that the ventral TP receives input within the visually associated precincts of the inferior temporal lobe, posited as the culmination point of visual processing. This alignment concurs with the decrement observed in the VBM values within this area in our investigation. This phenomenon is likely attributable to the impairment of visual processing in individuals with DVH, subsequently affecting the TP region associated with visual processing. Owing to its anatomical disposition, the TP actively engages in emotional responses and assumes a regulatory role in systemic emotional function[23]. Empirical studies consistently affirm that the right TP is instrumental in forging connections between autobiographical memory and sophisticated sensory representations, thereby playing a pivotal role in the storage of personal episodic memories[19]. Consequently, its diminution or loss not only profoundly impacts the recognition of familiar or renowned countenances, but also perturbs a spectrum of social and emotional functions encompassing subjective perception, anxiety, and stress[19-20,24]. Our current investigation delineates a diminished VBM value in the right superior temporal pole concomitant with an elevated HADS score in individuals afflicted with VDH. This implies a proclivity for intricate social and emotional dysfunctions and memory impairments when the TP is compromised. These impediments may manifest as depressive states, apathy, diminished communicative prowess, and attenuated social engagement with acquaintances. Consequently, this underscores the imperative in clinical practice to vigilantly monitor alterations in the mood of patients, in addition to assessing changes in their visual function.

The temporal lobe constitutes a pivotal element in the nuanced processing of elevated visual and auditory perception, intertwined with reward mechanisms[25]. The existing body of research predominantly explores temporal lobe dysfunction within the context of mood disorders. Notably, individuals afflicted with temporal lobe epilepsy exhibit a heightened propensity for despondency compared to counterparts with alternative forms of epilepsy[26]. Given its incorporation into the "Wernicke area," the superior temporal gyrus assumes a paramount role in language comprehension. It merits attention that within this region, human responses to visual, auditory, and somatosensory stimuli manifest a convergence[27]. Furthermore, the superior temporal gyrus actively engages in emotional processing and social cognition, concomitantly involving the orbital frontal cortex and the frontal marginal region of the amygdala[28]. For instance, Li *et al*[29] discerned this phenomenon in the cortices of individuals grappling with severe and major depressive disorders. A corpus of scholarly works attests that even with sustained usage of antipsychotic medications for mental health management, the gray matter volume of the superior temporal gyrus exhibits a persistent decline[30]. The right superior temporal gyrus is intricately associated with social cognitive functions, encompassing theory of mind, biological motion perception, and voice recognition[31]. Previous investigations have ascertained a reduction in gray matter volume within this gyrus among patients contending with retinal detachment[32]. Our inquiry similarly reveals a diminished VBM value in the right superior temporal gyrus, indicative of compromised vision in patients afflicted by DVH. Simultaneously, given its relevance to auditory perception, somatosensory reactions, and mood disorders, the HADS scores among DVH patients surpass those of individuals with uncomplicated diabetes. Moreover, we posit that the impediments in the daily activities of DVH patients may not solely emanate from compromised visual function. Rather, it is plausible that the occurrence of DVH precipitates damage to the patient's superior temporal gyrus, thereby instigating a cascade of adverse effects, including impaired vision, negative emotional states, and even auditory impairment in DVH patients.

The OFC, delineated by its anatomic situation on the medial aspect of the prefrontal cortex, is situated beneath the anterior cingulate and positioned superior to the ocular organs. The medial and lateral divisions manifest markedly distinct functions, engaged in reward and emotional processes and non-reward or punitive responses, respectively[33]. Nevertheless, over an extended temporal expanse, scholarly inquiries into this locale have predominantly focused on the realm of psychological infirmity. Exempli gratia, the volumetric extent of the medial orbitofrontal lobe, its responsiveness, and its functional interconnections with other encephalic regions are conspicuously diminished in subjects afflicted by melancholia[34-35]. Investigations involving primates, as conducted by Rolls *et al*[36-37], discern that the OFC, concomitant with the temporal lobe, is proficient in the reprocessing of assimilated information, facilitating the advancement and metamorphosis of perspectives, and assumes

the role of a receptive visage during the course of visual processing. This role finds manifestation in the semblance and articulation of its function. In congruence with these findings, this inquiry establishes that the VBM metric pertaining to the right medial orbital frontal lobe in individuals afflicted by DVH is diminished. This explication posits that DVH patients, in addition to experiencing mere ocular impairment, suffer compromise in their capacity for viewpoint processing, visual assimilation, and the reception of visual information. Therein lies the implication that, in the clinical milieu, metrics beyond the patient's visual acuity merit discernment. Furthermore, the elevated levels of anxiety and depression discernible in DVH patients may be attributed to the detriment incurred by the right medial orbital frontal lobe, attenuating the brain's reward mechanisms and rendering patients more susceptible to states of anxiety and despondency.

According to Brodmann's delineation, the lateral and superior segments of area 9, the entirety of area 8, and the outer expanse of area 6 collectively constitute the SFG situated in the elevated domain of the prefrontal cortex[38]. The frontal cortex assumes paramount importance in organizational proficiency, strategic planning, consideration of prospective repercussions, and the inhibition of impulsive tendencies[39]. Within this context, the functions of the SFG and the default mode network (DMN), the evolution of linguistic competencies encompassing reading and spelling proficiencies, intellectual acumen, and attentive faculties, motoric undertakings, social perceptiveness, and the regulation of emotional responses are intricately interconnected[38]. The left SFG additionally contributes to the amalgamation and retention of visual data and cognitive imagery, undertaking sophisticated roles inclusive of working memory functions, temporal processing, spatial representation, or manipulation[40-42]. Multiple investigations[43-46] have substantiated that conditions such as depression, Parkinson's disease, Alzheimer's disease, schizophrenia, attention deficit hyperactivity disorder, and other afflictions significantly impinging upon cognitive capacities entail deleterious alterations in the left upper frontal lobe. Our findings substantiate the outcomes of these investigations. Specifically, our study discerns that individuals afflicted with DVH exhibit diminished volumetric values in the left upper frontal lobe, concomitant with elevated HADS scores in comparison to the control group with normal visual perception. Hence, we postulate that the compromise of the SFG in DVH patients extends beyond mere visual acuity reduction, encompassing attenuation in visual information integration proficiency, working memory, spatial integration capabilities, and sophisticated social functions. Furthermore, with the progression of the ailment, our study reveals a concomitant reduction in VBM values within the SFG, indicating a heightened detriment to this cerebral region. Correspondingly, an escalation in HADS scores is noted. This prompts us to surmise that the advancing stages of DVH increasingly jeopardize the quality of life and physical well-being of afflicted individuals. Consequently, this underscores the imperative for timely and efficacious intervention in DVH, as it holds the potential not only to ameliorate visual function but also to profoundly impact the enduring quality of life for these patients.

In conclusion, as aforementioned, this investigation reveals that the cumulative decrement in VBM indices within four distinct cerebral regions among individuals afflicted with DVH not only manifests aberrations in visual acuity but also signifies anomalous alterations in the cerebral cortex, concomitant with diverse sensory functions. This prompts conjecture that, even when DVH is discerned at its incipient or mild stages and vision is subsequently reinstated through efficacious interventions, the corresponding cerebral cortex has already undergone protracted and broad-ranging pathological developments. Such protracted cortical modifications may instigate secondary afflictions, including but not limited to depressive disorders, in DVH-afflicted individuals. The etiology of this malady exerts a sustained influence on both the physiological and psychological well-being of the patient. These revelations furnish compelling substantiation for delving into the neuropathological underpinnings of DVH.

Owing to the constrained cohort aligning with the stipulated inclusion criteria, the study's sample size was notably diminutive. Nevertheless, DVH consistently advances in a continuous trajectory, exerting discernible influences on alterations in patients' vision. This inevitably prompts us to scrutinize potential disparities in disease progression and the inadvertent introduction of temporal errors during the screening process. Additionally, some confounding factors such as lifestyle factors and comorbid conditions, which could potentially affect brain morphology, were not considered.

Pathological alterations in four distinct brain regions were observed in patients with DVH, potentially reflecting neuropathological changes associated with this condition. We included both right eye and left eye injury patients, which might affect the VBM findings. Future studies should Increase sample size to distinguish the difference and measure brain function activity changes more accurately. Meanwhile, envisage a broader exploration across both the horizontal and vertical dimensions of the study. This could include potential interventions that could mitigate these brain changes.

ACKNOWLEDGEMENTS

Foundations: Supported by National Natural Science Foundation of China (No.82160195; No.82460203); Science and Technology Project of Jiangxi Provincial Department of

Education (No.GJJ200169); Science and Technology Project of Jiangxi Province Health Commission of Traditional Chinese Medicine (No.2020A0087); Science and Technology Project of Jiangxi Health Commission (No.202130210).

Conflicts of Interest: Ji LJ, None; **Hu JY,** None; **Zeng YM,** None; **Ling Q,** None; **Zou J,** None; **Chen C,** None; **He LQ,** None; **Wang XY,** None; **Wei H,** None; **Chen X,** None; **Wang YX,** None; **Shao Y,** None; **Yu Y,** None.

REFERENCES

1 Confalonieri F, Barone G, Ferraro V, *et al*. Early versus late pars Plana vitrectomy in vitreous hemorrhage: a systematic review. *J Clin Med* 2023;12(20):6652.

2 Qin YW, Zhang J, Babapoor-Farrokhran S, *et al*. PAI-1 is a vascular cell-specific HIF-2-dependent angiogenic factor that promotes retinal neovascularization in diabetic patients. *Sci Adv* 2022;8(9):eabm1896.

3 Zhang YQ, Zhu FY, Tang LY, *et al*. Altered regional homogeneity in patients with diabetic vitreous hemorrhage. *World J Diabetes* 2020;11(11):501-513.

4 Ren JH, Zhang SX, Pan YF, *et al*. Diabetic retinopathy: Involved cells, biomarkers, and treatments. *Front Pharmacol* 2022;13:953691.

5 Semeraro F, Morescalchi F, Cancarini A, *et al*. Diabetic retinopathy, a vascular and inflammatory disease: Therapeutic implications. *Diabetes Metab* 2019;45(6):517-527.

6 Huang X, Zhang Q, Hu PH, *et al*. White and gray matter volume changes and correlation with visual evoked potential in patients with optic neuritis: a voxel-based morphometry study. *Med Sci Monit* 2016;22:1115-1123.

7 Straub J, Brown R, Malejko K, *et al*. Adolescent depression and brain development: evidence from voxel-based morphometry. *J Psychiatry Neurosci* 2019;44(4):237-245.

8 Hirakawa N, Kuga H, Hirano Y, *et al*. Neuroanatomical substrate of chronic psychosis in epilepsy: an MRI study. *Brain Imaging Behav* 2020;14(5):1382-1387.

9 Takano Y, Tatewaki Y, Mutoh T, *et al*. Voxel-based morphometry reveals a correlation between bone mineral density loss and reduced cortical gray matter volume in Alzheimer's disease. *Front Aging Neurosci* 2020;12:178.

10 Yang ZY, Wang SK, Li Y, *et al*. Neural correlates of prospection impairments in schizophrenia: Evidence from voxel-based morphometry analysis. *Psychiatry Res Neuroimaging* 2019;293:110987.

11 Cheng KL, Lin LH, Chen PC, *et al*. Reduced gray matter volume and risk of falls in Parkinson's disease with dementia patients: a voxel-based morphometry study. *Int J Environ Res Public Health* 2020;17(15):5374.

12 Kristiansen M, Lindén C, Qvarlander S, *et al*. Feasibility of MRI to assess differences in ophthalmic artery blood flow rate in normal tension glaucoma and healthy controls. *Acta Ophthalmol* 2021;99(5):e679-e685.

13 Huang J, Duan YY, Liu SD, *et al*. Altered brain structure and functional connectivity of primary visual cortex in optic neuritis. *Front Hum Neurosci* 2018;12:473.

14 Peng JX, Yao F, Li QY, *et al*. Alternations of interhemispheric functional connectivity in children with strabismus and amblyopia: a resting-state fMRI study. *Sci Rep* 2021;11(1):15059.

15 Shao Y, Li QH, Li B, *et al*. Altered brain activity in patients with strabismus and amblyopia detected by analysis of regional homogeneity: a resting-state functional magnetic resonance imaging study. *Mol Med Rep* 2019;19(6):4832-4840.

16 Shi WQ, He Y, Li QH, *et al*. Central network changes in patients with advanced monocular blindness: a voxel-based morphometric study. *Brain Behav* 2019;9(10):e01421.

17 Lan DY, Zhu PW, He Y, *et al*. Gray matter volume changes in patients with acute eye pain: a voxel-based morphometry study. *Transl Vis Sci Technol* 2019;8(1):1.

18 Ge QM, Shen YK, Pan YC, *et al*. Decreased gray matter volume and increased white matter volume in patients with neovascular age-related macular degeneration: a voxel-based morphometry study. *Aging* 2021;13(19):23182-23192.

19 Herlin B, Navarro V, Dupont S. The temporal pole: From anatomy to function-a literature appraisal. *J Chem Neuroanat* 2021;113:101925.

20 Mesulam MM. Temporopolar regions of the human brain. *Brain* 2023;146(1):20-41.

21 Rolls ET, Deco G, Huang CC, *et al*. The human language effective connectome. *Neuroimage* 2022;258:119352.

22 Martin CB, Douglas D, Newsome RN, *et al*. Integrative and distinctive coding of visual and conceptual object features in the ventral visual stream. *eLife* 2018;7:e31873.

23 Qiu ZG, Lei X, Becker SI, *et al*. Neural activities during the Processing of unattended and unseen emotional faces: a voxel-wise Meta-analysis. *Brain Imaging Behav* 2022;16(5):2426-2443.

24 Sonkusare S, Nguyen VT, Moran R, *et al*. Intracranial-EEG evidence for medial temporal pole driving amygdala activity induced by multi-modal emotional stimuli. *Cortex* 2020;130:32-48.

25 Steel A, Silson EH, Stagg CJ, *et al*. Differential impact of reward and punishment on functional connectivity after skill learning. *Neuroimage* 2019;189:95-105.

26 Sair A, Şair YB, Saracoğlu İ, *et al*. The relation of major depression, OCD, personality disorders and affective temperaments with Temporal lobe epilepsy. *Epilepsy Res* 2021;171:106565.

27 Mesulam MM, Rader BM, Sridhar J, *et al*. Word comprehension in temporal cortex and Wernicke area: a PPA perspective. *Neurology* 2019;92(3):e224-e233.

28 Chauhan P, Rathawa A, Jethwa K, *et al*. The anatomy of the cerebral cortex. *Cerebral Ischemia* 2021:1-16.

29 Li HR, Zhang HW, Yin L, *et al*. Altered cortical morphology in major depression disorder patients with suicidality. *Psychoradiology* 2021;1(1):13-22.

30 Gong QY, Lui S, Sweeney JA. A selective review of cerebral abnormalities in patients with first-episode schizophrenia before and after treatment. *Am J Pcychiatry* 2016;173(3):232-243.

31 Kobayashi A, Yokota S, Takeuchi H, *et al*. Increased grey matter volume of the right superior temporal gyrus in healthy children with autistic cognitive style: a VBM study. *Brain Cogn* 2020; 139:105514.

32 Li B, Liu YX, Li HJ, *et al*. Reduced gray matter volume in patients with retinal detachment: evidence from a voxel-based morphometry study. *Acta Radiol* 2020;61(3):395-403.

33 Rolls ET. The orbitofrontal cortex. *Philos Trans R Soc Lond B Biol Sci* 1996;351(1346):1433-1443;discussion 1443-1444.

34 Rolls ET, Cheng W, Gilson M, *et al*. Effective connectivity in depression. *Biol Psychiatry Cogn Neurosci Neuroimaging* 2018;3(2):187-197.

35 Rolls ET, Cheng W, Feng JF. The orbitofrontal cortex: reward, emotion and depression. *Brain Commun* 2020;2(2):fcaa196.

36 Rolls ET. The orbitofrontal cortex and emotion in health and disease, including depression. *Neuropsychologia* 2019;128:14-43.

37 Rolls ET. The cingulate cortex and limbic systems for emotion, action, and memory. *Brain Struct Funct* 2019;224(9):3001-3018.

38 Jung J, Lambon Ralph MA, Jackson RL. Subregions of DLPFC display graded yet distinct structural and functional connectivity. *J Neurosci* 2022;42(15):3241-3252.

39 Snelleksz M, Rossell SL, Gibbons A, *et al*. Evidence that the frontal pole has a significant role in the pathophysiology of schizophrenia. *Psychiatry Res* 2022;317:114850.

40 Qiu LL, Yan H, Zhu RS, *et al*. Correlations between exploratory eye movement, hallucination, and cortical gray matter volume in people with schizophrenia. *BMC Psychiatry* 2018;18(1):226.

41 Ren ZT, Zhang Y, He H, *et al*. The different brain mechanisms of object and spatial working memory: voxel-based morphometry and resting-state functional connectivity. *Front Hum Neurosci* 2019;13:248.

42 Jenkins LM, Bodapati AS, Sharma RP, *et al*. Working memory predicts presence of auditory verbal hallucinations in schizophrenia and bipolar disorder with psychosis. *J Clin Exp Neuropsychol* 2018;40(1):84-94.

43 Kang SG, Cho SE, Na KS, *et al*. Differences in brain surface area and cortical volume between suicide attempters and non-attempters with major depressive disorder. *Psychiatry Res Neuroimaging* 2020;297:111032.

44 Xu YQ, Yang J, Hu XY, *et al*. Voxel-based meta-analysis of gray matter volume reductions associated with cognitive impairment in Parkinson's disease. *J Neurol* 2016;263(6):1178-1187.

45 Fujimoto H, Matsuoka T, Kato Y, *et al*. Brain regions associated with anosognosia for memory disturbance in Alzheimer's disease: a magnetic resonance imaging study. *Neuropsychiatr Dis Treat* 2017;13:1753-1759.

46 Ding YD, Ou YP, Su QJ, *et al*. Enhanced global-brain functional connectivity in the left superior frontal gyrus as a possible endophenotype for schizophrenia. *Front Neurosci* 2019;13:145.